AD-A169 138 ELECTROCHEMISTRY IN NEAR-CRITICAL AND SUPERCRITICAL FLUIDS 3 STUDIES OF B.. (U) TEXAS UNIV AT AUSTIN DEPT OF CHEMISTRY W M FLARSHEIM ET AL. FEB 86 TR-3 1/1

UNCLASSIFIED N00014-84-K-0428 F/G 7/4 NL

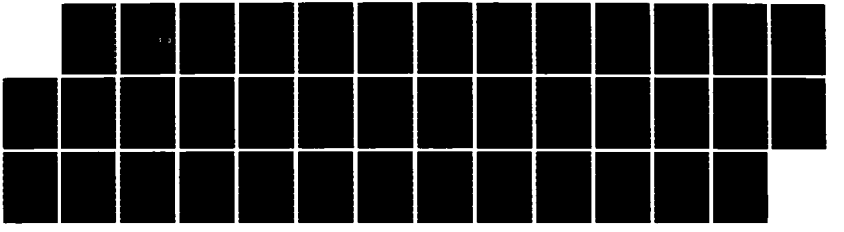

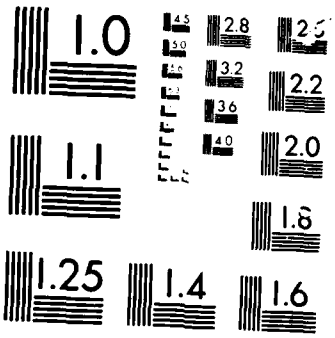
1.0
1.1
1.25
1.4
1.6
1.8
2.0
2.2
2.8
3.2
3.6
4.0

(12)

OFFICE OF NAVAL RESEARCH

Contract N00014-84-K-0428

Task No. NR 051-693

TECHNICAL REPORT No. 3

Electrochemistry in Near-Critical and Supercritical Fluids. 3. Studies of $Br^-_{(1)}$, $I^-_{(1)}$, and Hydroquinone in Aqueous Solutions

By

William M. Flarsheim*, Yu-Min Tsou*, Isacc Trachtenberg*,
Keith P. Johnson*, Allen J. Bard*

Prepared for Publication

in

Journal of Physical Chemistry

The University of Texas at Austin
Department of Chemistry
Austin, Texas 78712

SECURITY CLASSIFICATION OF THIS PAGE (When Data Entered)

REPORT DOCUMENTATION PAGE

READ INSTRUCTIONS BEFORE COMPLETING FORM

1. REPORT NUMBER: 3	2. GOVT ACCESSION NO.: AD-A169138
3. RECIPIENT'S CATALOG NUMBER:	
4. TITLE (and Subtitle): Electrochemistry in Nearcritical and Supercritical Fluids. 3. Studies of Br^-, I^-, and Hydroquinone in Aqueous Solutions	5. TYPE OF REPORT & PERIOD COVERED:
	6. PERFORMING ORG. REPORT NUMBER:
7. AUTHOR(s): William M. Flarsheim, Yu-Min Tsou, Isacc Trachtenberg, Keith P. Johnson and Allen J. Bard	8. CONTRACT OR GRANT NUMBER(s): N00014-84-K-0428
9. PERFORMING ORGANIZATION NAME AND ADDRESS: Department of Chemistry, University of Texas at Austin, Austin, TX 78712	10. PROGRAM ELEMENT, PROJECT, TASK AREA & WORK UNIT NUMBERS:
11. CONTROLLING OFFICE NAME AND ADDRESS: Office of Naval Research, 800 N. Quincy, Arlington, VA 22217	12. REPORT DATE:
	13. NUMBER OF PAGES:
14. MONITORING AGENCY NAME & ADDRESS (if different from Controlling Office):	15. SECURITY CLASS. (of this report): Unclassified
	15a. DECLASSIFICATION/DOWNGRADING SCHEDULE:

16. DISTRIBUTION STATEMENT (of this Report)

This document has been approved for public release and sale; its distribution is unlimited.

17. DISTRIBUTION STATEMENT (of the abstract entered in Block 20, if different from Report)

18. SUPPLEMENTARY NOTES

Prepared for publication in the Journal of

19. KEY WORDS (Continue on reverse side if necessary and identify by block number)

Electrochemistry, Hydroquinone

20. ABSTRACT (Continue on reverse side if necessary and identify by block number) A new type of apparatus has been constructed for carrying out electrochemistry in nearcritical and supercritical aqueous solutions. The following systems have been studied at a platinum electrode: H_2O/O_2, I^-/I_2, Br^-/Br_2, and hydroquinone/benzoquinone. The compact, alumina flow-cell can be heated or cooled quickly, and can be recharged with fresh electrolyte solution while at high temperature and pressure. A large reduction in the potential required for the electrolysis of water was observed. Diffusivities have been measured for iodide ions and hydroquinone. General agreement with the Stokes-Einstein model was observed in the temperature range 25°C to 375°C.

DD FORM 1 JAN 73 1473 EDITION OF 1 NOV 65 IS OBSOLETE
S/N 0102-014-6601

Unclassified
SECURITY CLASSIFICATION OF THIS PAGE (When Data Entered)

ELECTROCHEMISTRY IN NEARCRITICAL AND SUPERCRITICAL FLUIDS. 3. STUDIES OF Br^-, I^-, AND HYDROQUINONE IN AQUEOUS SOLUTIONS.

William M. Flarsheim*, Yu-Min Tsou+, Isaac Trachtenberg*,
Keith P. Johnston*, Allen J. Bard+,
Departments of Chemical Engineering* and Chemistry+.
The University of Texas,
Austin, TX 78712

(Abstract)

A new type of apparatus has been constructed for carrying out electrochemistry in nearcritical and supercritical aqueous solutions. The following systems have been studied at a platinum electrode: H_2O/O_2, I^-/I_2, Br^-/Br_2, and hydroquinone/benzoquinone. The compact, alumina flow-cell can be heated or cooled quickly, and can be recharged with fresh electrolyte solution while at high temperature and pressure. A large reduction in the potential required for the electrolysis of water was observed. Diffusivities have been measured for iodide ions and hydroquinone. General agreement with the Stokes-Einstein model was observed in the temperature range 25°C to 375°C.

(End of abstract)

Submitted to the Journal of Physical Chemistry
December 1985
Revised February 1986

I. Introduction

Nearcritical and supercritical water holds great promise as a solvent because it can dissolve non-polar organic compounds and polar inorganic salts simultaneously. This makes it possible to develop electro-organic syntheses in water, instead of in an expensive and possibly toxic organic solvent. We have designed an electrochemical cell that can be operated above the critical point of water (T_c = 374°C, P_c = 221 bar). Areas of investigation reported here include the effect of temperature on redox potentials, electrode kinetics (i.e. overpotentials), mass transport rates, and other electrochemical parameters.

Research in the area of supercritical fluids has been expanding in recent years, primarily because of an awareness of the unique solvent properties of materials in the critical region. Gases such as carbon dioxide and ethylene have been used as solvents for extraction, and in a variety of other manufacturing processes.[1-3] However, water the most readily available and used solvent has received very little attention as a supercritical solvent, perhaps because of its relatively high critical temperature and critical pressure.

At high temperature, particularly as the critical temperature is approached, the hydrogen bonding that exists in water at lower temperature is diminished.[4] The dielectric constant decreases so that the resulting solvent properties make near-critical and supercritical water a promising medium for a variety of chemical and electrochemical processes. Super-

critical water has been used as a medium for the liquefaction and extraction of coal,[5] tar sands,[6] and biomass.[7] Complete oxidation of most organic pollutants has also been achieved in a mixture of supercritical water and air.[8] There is significant ongoing research in the electrochemistry of metals in high temperature aqueous solutions, because of its importance to the electric power and metal manufacturing industries.[9]

This work is part of a continuing study of electrochemistry in near- and supercritical fluids.[10,11] A previous study of aqueous solutions[10] employed a quartz electrochemical cell contained in a steel bomb. The electrochemistry of some supporting electrolyte solutions was studied. In addition, the diffusivity of Cu^{2+} was measured up to 245°C.

Though it did yield useful results, this initial work was hampered by experimental difficulties that arose from using a large pressure vessel to contain the cell. The main disadvantage was the inability to recharge the cell with fresh electrolyte solution while at high temperature. If the electrolyte solution became degraded for any reason (e.g. a current overload caused by overcompensation of resistance), a complete shutdown of the system was necessary. A lengthy experimental delay resulted from the long setup, heating, and cooling time necessary for the 12 kg bomb. Other problems arose from the high temperature seals around the electrode, the large amount of energy stored in the heated bomb, contact between the electrolyte and the steel walls at temperatures above the critical point, and possible contamination of the solution by

products formed at the counter electrode.

The new electrochemical cell presented here addresses each of these drawbacks in the previous design. A High Pressure Liquid Chromatography (HPLC) pump is used to introduce fresh solution at operating conditions. The small volume of heated solution permits rapid heating and cooling of the cell, so that measurements can be made at more temperatures in a single experimental run. Because of the small volume, experiments can be conducted behind a Plexiglass shield instead of a cinder block wall. The electrodes feedthroughs are at a low temperature, so that Teflon seals can be used. The alumina pressure vessel has greatly reduced problems arising from corrosion.

II. Experimental Section.

Apparatus. A diagram of the high pressure and temperature electrochemical cell is shown in Figure 1. The key element is the cell body, a 0.635 cm (1/4") O.D. by 0.238 cm (3/32") I.D., 15 cm (6") long alumina tube (99.8% Al_2O_3), that contains the pressurized solution at high temperature. Al_2O_3 was chosen to avoid corrosion and spurious electrical fields within the cell. Only the central portion of the tube is heated. All pressure seals are located at the relatively cool end fittings. This permits the use of Teflon (poly-tetrafluoroethylene, TFE) as the sealing material. The connections for the alumina tube are steel Swagelok fittings with TFE ferrules. The electrode leads pass through compression fittings consisting of a TFE disk

between two alumina washers. The lengths of the working and reference electrodes were tailored such that the tip-to-tip distance was less than 1.3 cm. All metal parts are either 316 stainless steel or Hastelloy Alloy C.

The complete experimental system is shown schematically in Figure 2. The system was pressurized with a Milton Roy (Riviera Beach, FL) Minipump (Model 396 Slow Speed). During measurements, the outlet valve was closed so that the solution was stationary at the electrode. A tube packed with 1 um alumina powder maintained the pressure while the cell was being recharged with fresh solution. Only deionized water was passed through the pump to protect it from corrosion. The electrolyte solutions were introduced using a Valco Instruments (Houston, TX) HPLC sample valve. A thermocouple cemented to the tube wall provided input to an Autoclave Engineers (Erie, PA) proportional-integral temperture controller (Model 520). The controller operates a nichrome wire heater wrapped around the 75 mm central portion of the alumina tube to regulate the cell temperature. The temperature was controlled to within 5°C and the pressure to within 2 bar of the desired values. The electrochemical cell has been operated at temperatures up to 400°C and pressures up to 270 bar. All of the data presented here are at 240 bar.

Procedure. The working electrodes were made by welding a spot of platinum to a tantalum wire. By oxidizing the electrode in sulfuric acid, a thick oxide layer was formed on the tantalum which passivated it completely. Thus only the platinum tip, which was within the hot zone of the cell, was active. The

electrode used for studing the cyclic voltammetry of I^-/I_2, Br^-/Br_2, and the $NaHSO_4$ supporting electrolyte solution had an area of 1.3×10^{-2} cm^2, and the electrode used to measure diffusion coefficients and the cyclic voltammetry of hydroquinone/benzoquinone had an area of 1.9×10^{-3} cm^2. The geometric areas were determined by measuring diffusion currents from chronoamperometric potential step experiments at 25°C in solutions of hydroquinone or KI in 0.2 M $NaSO_4$. Kolthoff and Orlemann have previously measured the diffusivity of hydroquinone in water as $7.4 \pm 0.2 \times 10^{-6}$ cm^2/sec at 25°C.[12] With this value as a standard, the diffusivity of iodide ions in water at 25°C was measured with a large platinum-in-glass electrode (area, 0.20 cm^2) and a three compartment cell. A value of $1.4 \pm 0.1 \times 10^{-5}$ cm^2/sec was obtained in 0.2 M $NaHSO_4$ supporting electrolyte solution. These values were also used as the basis for calculating the diffusivity at high temperature. Before each set of experiments, the electrode was held at +10V in 2M H_2SO_4 for 20 seconds. This treatment refreshed the tantalum oxide layer and exposed a clean, active surface on the platinum, and resulted in reproducible behavior.

A silver wire was used as a quasireference electrode. The silver was connected to a tantalum lead with a small bridge of platinum. As with the working electrode, the tantalum was coated with oxide. A stable potential was obtained in all solutions. The auxiliary electrode was a platinum wire (exposed area, 0.47 cm^2) located in the downstream endblock of the cell.

For cyclic voltammetry and chronoamperometry, a Princeton

Applied Research Model 173/179 potentiostat/digital coulometer with a Model 175 universal programmer was employed. Positive feedback was used to compensate for solution resistance. Because the tantalum reference electrode lead has a large capacitance, it was not always possible to compensate fully for the solution resistance. The current and potential data were recorded with a Norland Model 3001 digital oscilloscope. For each measurement 1024 data points were recorded. The sampling rate was 1.0 msec for recording cyclic voltammograms and 0.1 msec for chronoamperometric experiments.

Chemicals were reagent grade and were used as received. Solutions were prepared from distilled water that was further treated by passage through a Millipore, Milli-Q Reagent Water System. All experiments were conducted in solutions that had been deaerated with nitrogen.

III. Results and Discussion

Supporting Electrolyte. Figure 3 shows a series of cyclic voltammograms of a 0.2 M $NaHSO_4$ solution, the supporting electrolyte for this study. In Figure 3, peak A is the current from the reduction of protons to hydrogen. Peak B is from the oxidation of water to oxygen. The voltage scales have been adjusted so that the potential of zero current on the hydrogen wave was defined as zero volts versus the reference. This potential is approximately 250 mV negative of the potential of a normal hydrogen electrode (NHE), because the pH of the bulk solution is about 1.4 (versus 0 in a NHE). The pH at the

electrode is slightly increased by the reduction of H^+ to H_2. As long as the same peak hydrogen current is reached in each voltammogram, the zero crossing point is a stable reference, that is especially convenient for higher temperature measurements. Since the zero current potential at the oxygen limit is not easily located, some other measure of the oxygen potential must be chosen. We have picked the potential where the current drops below 130 μA (10 mA/cm^2) after the potential sweep is reversed. Though this choice is somewhat arbitrary, the varition of this potential with temperature provides information related to the redox potential and the overpontial characteristics of the H_2O/O_2 system.

As seen in previous studies, the potential window between hydrogen and oxygen evolution narrows with an increase in temperature. The change in potential window was monitored from 25°C to 390°C and the results are plotted in Figure 4. The total decrease in the potential required for the electrolysis of water is 410 mV as the temperature is increased from 25°C to 350°C. Of this 410 mV decrease, approximately 100 mV can be attributed to the decrease in the free energy required to split water.[13] The major component of the shift is presumably a decrease in the oxygen overpotential on platinum. This reduction in voltage is the result of the high overpotential for the oxygen evolution reaction on platinum at room temperature.[14] The effect of temperature on H_2O electrolysis has been studied previously.[15] but, to the authors' knowledge, has not been previously reported over such a broad temperature range.

In addition to the change in potential window, the other significant feature of the cyclic voltammograms was observed in the waves from oxidation and reduction of the platinum surface (peaks C and D) in Figure 3. These have been the subject of a number of previous studies.[16] At 25°C the oxidation of the Pt surface to an oxide or adsorbed oxygen species occurs in a broad, drawn out anodic wave (C) that precedes oxygen evolution. Reduction of the electrode surface occurs at a better-defined peak (D).

Above 100°C, a more pronounced peak develops. The oxidation peak sharpens with increasing temperature, a consequence of the increasing reaction rate. Also, as the kinetic rate increases, the overpotential necessary to drive the reaction declines. Thus, the potential gap between the oxidation and reduction waves decreases with increasing temperature. By averaging the peak potentials of waves C and D at 200°C, we can estimate a potential of 0.87 V for the Pt surface oxide redox process.

An unusual feature of Figure 3 is the anodic peak in the negative scan at 375°C and 390°C. In preliminary experiments with sodium acetate, phenol, and benzene, this behavior has been observed at temperatures as low as 250°C. For this reason, we believe that this anodic peak is the result of an organic impurity in the cell. The impurity did not interfere with the measurement of the anodic and cathodic limits of the solution, which was the main thrust of this series of experiments. Thoroughly cleaning the cell eliminated this behavior from later

experiments.

Redox Reactions: KI and KBr. As an initial study of high temperature electrochemistry the halogen couples I^-/I_2 and Br^-/Br_2 were examined with cyclic voltammetry. Representative cyclic voltammograms (CV's) are shown in Figures 5 and 6. These redox couples were chosen because they are known to exhibit rapid kinetics on a platinum electrode at 25°C, and neither halide was expected to undergo any further reaction in the potential range examined, even at high temperature.

From a qualitative standpoint, the CV's of the KI solution show no dramatic changes up to 390°C. The iodine reduction wave, peak B, is distorted at 25°C because iodine is **insoluble** at this concentration of I^- and precipitates on the electrode surface. This does not persist to higher temperature. There is an increase in peak current because of higher diffusion rates at higher temperature. This trend is partially offset because the concentration of iodide at the electrode is reduced by solution expansion. The solution expands 100% between 25°C and 375°C.

At 350°C and above, the CV's are slightly distorted. They do not show the nernstian behavior seen at lower temperatures. This is not a characteristic of the I^-/I_2 couple, but the result of uncompensated solution resistance. As mentioned above, the amount of positive feedback compensation that can be used is limited by the cell design. The conductance of a 0.2 M Na_2SO_4 solution dropped sharply above 300°C, as has been observed by others in similar experiments[17].

The cyclic voltammograms of the KBr solution are slighty

more complicated than those of KI because of interference from the surface oxidation of platinum and the oxidation of water. The first complication can be overcome by studing the Br^-/Br_2 couple on a fully oxidized electrode. Figure 6 contains two sets of cyclic voltammograms. One shows a complete scan from the hydrogen to the oxygen limits of the solution (dashed line). Also plotted are voltammograms that center on the Br^-/Br_2 couple (solid line). This second set was made by scanning positive from the initial potential to the anodic solution limit, negative, over the bromine reduction wave, and then reversing and scanning positive without reducing the platinum surface. The oxidation of bromide is peak A, the reduction of bromine is peak B, the oxidation and reduction of the platinum electrode occurs in peak C and D respectively, and peak E is the oxidation of water to hydrogen.

At low temperature, the Br^-/Br_2 wave (see solid line in Figure 6) has the characteristic nernstian shape. As the temperature is increased, the shifting oxygen limit of the solution distorts the shape. Above 250°C, it is no longer possible to discern an oxidation peak for bromide, only a shoulder at the anodic solution limit. At 375°C, neither the oxidation or the reduction wave for bromine can be seen in the CV. It is completely hidden by water oxidation and reactions affecting the platinum surface.

The variations in redox potentials of the I^-/I_2 and Br^-/Br_2 couples with temperature are shown in Figure 4. The redox potentials were determined by averaging the peak potential of

the oxidation and reduction waves in each cyclic voltammogram. As mentioned above, the potentiostat could not fully compensate for solution resistance at high temperature. This affects the peak potentials. However the digitized voltammograms, obtained with the Norland oscilloscope, could be adjusted (numerical positive feedback resistance compensation) to eliminate the effect of resistance on the measured potentials. The amount of compensation added was determined as follows. In the absence of solution resistance, a nernstian couple such as I^-/I_2 will show a peak separation of about 2.3RT/nF, where R is the gas constant, n is the number of electrons, and F is the Faraday constant. The peak separation was measured on each CV, and compared to the nernstian value at the temperature. These data are shown in Figure 7. The sum of the anodic and cathodic peak current was also measured. The voltage difference between the actual peak separation and the nernstian peak separation, divided by the peak to peak current gives an estimate of the uncompensated resistance. The CV's were then digitally corrected for this resistance, and the redox potentials measured on a resistance free basis. The only redox potentials affected by this procedure were the values for I^-/I_2 at 350°C, 375°C, and 390°C, where the uncompensated resistance was 150, 180, and 250 ohms, respectively.

Up to 250°C, there is little change in the redox potential of either I^-/I_2 or Br^-/Br_2. The dielectric constant of water drops from 78 at 25°C to 28 at 250°C. Apparently, the change in the solvation energy of these halide ions is small compared to

the overall free energy of reaction.

Above 250°C it is not possible to determine a redox potential for bromine from the cyclic voltammograms, as discussed above. The redox potential of iodine begins to change noticeably above 250°C, and drops sharply above 350°C. The 150 mV change between 350°C and 390°C corresponds to a drop of 3.5 kcal in the free energy change of the reaction

$$I^-(aq) + H^+(aq) \rightleftharpoons 1/2I_2 + 1/2H_2$$

We suggest that the potential shift is probably the result of a drop in solvation energy for the ionic species. The dielectric constant of water drops from 15 at 350°C to 3 at 390°C. Using the radius of I^- calculated from its diffusivity (see below), the Born model predicts that aqueous I^- will be destabilized by 2.5 kcal when the temperature is raised from 350°C to 390°C, which is consistent with the data.

Hydroquinone. Solutions of organic species in supercritical water have been studied by a number of investigators,[18,19] and alkanes, aromatics, and other simple molecules are reported to be stable if oxygen is excluded. A mixture of air and supercritical water will completely oxidize a variety of organics at 375°C.[8] These studies indicate that at high temperatures, organic compounds will be stable at some potentials, but will decompose on an electrode as the potential approaches that of oxygen evolution.

Since organic compounds are expected to exhibit novel electrochemistry at high temperatures, we included an organic redox couple in this initial study. The

hydroquinone/benzoquinone couple was chosen because the high solubility of hydroquinone in water at 25°C made it possible to study the couple over the entire temperature range of the apparatus. The cycle voltammograms obtained are shown in Figure 3.

The significant result of this study is that the hydroquinone/benzoquinone couple is stable in water up to its critical point, and can be studied with conventional electrochemical techniques. This gives us confidence that it will be possible to study a wide variety of organic compounds under these conditions. Above 250°C, benzoquinone was observed to decompose near the anodic limit of the solution, but as long as this region is avoided, it should be possible to exploit the increased solubility of organics in high temperature water to develop new electrochemical syntheses.

Diffusivities of Iodide and Hydroquinone. Chronoamperometry was employed to measure the diffusivities of iodide and hydroquinone. The measurements were made as follows. In a solution of KI or hydroquinone, the working electode is set at a potential where the reduced species is stable. The potential of the electrode is stepped, so that at the new potential, the redox species is fully oxidized on the electrode. The current that flows is determined by the rate at which I^- or hydroquinone diffuses to the electrode.

The oxidation of I^- may proceed directly to I_2,

$$2I^- \rightarrow I_2 + 2e^-$$

or through the intermediate I_3^-.

$$I_2 + I^- \rightleftharpoons I_3^-$$

$$2I_3^- \rightarrow 3I_2 + 2e^-$$

The formation of I_3^-, which has a lower diffusion coefficient than I^-,[20] will reduce the measured current, and thus the measured diffusivity. Toren and Driscoll have shown that in solutions that initially contain only I^-, this effect is small,[21] and will be negligible with respect to the temperature induced change in the diffusion coefficient reported here.

For a planar electrode, the diffusion equation can be solved analytically. The current measured is given by the Cottrell equation[22]

$$i = nFAD^{1/2}C/(\pi t)^{1/2}$$

where n is the number of electrons per species oxidation, F is the Faraday constant, A is the electrode area, D is the diffusion coefficient, C is the concentration of the reduced species, and t is time. The diffusion coefficient was obtained from a plot of i versus $t^{-1/2}$. Since the current measured can be affected by extraneous processes, both faradaic and non-faradaic, better results were obtained by taking the difference between slopes measured at two different concentrations. When measuring the diffusion coefficient of hydroquinone, 0.5 mM KCl was added to the solution. This helped stabilize the reference electrode, so that the measurements made at two different concentrations of hydroquinone could be more easily compared. A more detailed description of this technique can be found in the literature.[22]

At high temperature, expansion of the solution results in a

drop in the concentration of the diffusing species. To account for this in calculating diffusivities, the volume of liquid water at high temperature and pressure was obtained from the ASME Steam Tables.[23] The measured diffusivities for iodide and hydroquinone are shown in Figures 9 and 10, along with the values predicted by the Stokes-Einstein model. The data are also presented in Tables 1 and 2.

The agreement between the data for iodide and that predicted from the Stokes-Einstein equation is within an average of 10%. From this we conclude that the size of the solvent sphere around the iodide ion does not change appreciably between 25°C and 375°C. The diameter calculated from the Stokes-Einstein equation is 1.8 Å. If desolvation of the ion had occurred as a result of increased thermal energy and decreasing density, the apparent size of the ion in solution would decrease. This would manifest itself as a positive deviation from the Stokes-Einstein model. The Stokes-Einstein model assumes that a liquid is continuous, not molecular, at the length scale of the diffusing species. It is applicable to most liquids when the density is relatively high, near the triple point density. In vapor systems, a theory based on mean free path molecular collisions is best for treating diffusion. These data show that a liquid theory of diffusion is appropriate for water at densities down to 0.5 g/cm^3, a reduced density of 1.6. Jonas has measured self-diffusion in D_2O, and found Stokes-Einstein behavior for densities above the critical density.[24]

Hydroquinone shows a positive deviation from the Stokes-

Einstein theory above 200°C. In terms of this hydrodynamic model, this implies that the apparent size of the molecule decreases, from an effective spherical diameter of 3.3 Å at 25°C to 2.4 Å at 300°C. A breakdown of the hydrogen bonds between hydroquinone and water is a possible mechanism for the decrease in size.

In a previous study,[10] it was found that the diffusivity of $Cu^{2+}_{(aq)}$ showed a large positive deviation from Stokes-Einstein theory. This was attributed to a change in solvation environment around Cu^{2+}. It could reflect a high charge density of Cu^{2+}, which induces a pronounced change in solvation environment, as the entropy increase resulting from release of water molecules from solvation sphere dominates the free energy change of the solvation process at high temperature. Compared with Cu^{2+}, I^- has a much lower charge density so that the solvation is not significant enough to show a detectable change in apparent ion diameter.

More studies are necessary to reveal all the factors influencing the solvation environment of a species in high temperature aqueous solution. For the above systems, the diffusivities of solutes in aqueous solution increase with temperature according to Stokes-Einstein theory, or exhibit a positive deviation due to desolvation.

IV. Conclusions.

The electrochemical flow-cell has been shown to operate reliably above the critical temperature of water. From the

experiments described in this paper, the following conclusions can be drawn:

An increase in temperature greatly accelerates the kinetics of oxygen evolution on platinum. This reduces the potential required for the electrolysis of water on platinum from 1.84 V at 25°C to 1.43 V at 390°C.

The redox potentials of ionic couples, specifically I^-/I_2, become very temperature sensitive in the critical region. This is attributed to a destablization of the ions because of the drop in the dielectric constant of water when approaching its critical point.

Organic compounds such as hydroquinone can be studied in near-critical and supercritical water. Hydroquinone retains its low temperature electrochemical behavior and shows no sign of decomposition at temperatures up to 375°C as long as the potential of the electrode is not driven to the anodic limit, where oxygen is evolved.

Diffusion rates are greatly enhanced by higher temperatures. The enhancement is primarily the result of reduced solution viscosity. The diffusivities of iodide ion and hydroquinone can be modelled by Stokes-Einstein diffusion theory.

Since the feasibility of electrochemistry in water near the critical point has been demonstrated, a study of organic reactions is being undertaken. Preliminary tests with acetic acid, phenol, methanol, and benzene show that these compounds can all be oxidized electrochemically above 250°C. To

facilitate the collection and analysis of reaction products, a larger electrochemical cell is being constructed. The results will be presented in forthcoming publications.

Acknowledgments.

WMF is grateful to The University of Texas Graduate School and the Shell Foundation for support. We are indebted to Alex McDonald for his contributions at the early stages of this work. This research was funded by the Office of Naval Research and The University of Texas Separations Research Program.

Table 2: Effect of Temperature on the Diffusion Coefficient of Hydroquinone.

T (°C)	Slope of Current vs. $(Time)^{-1/2}$ (ampere/second$^{1/2}$ × 10^2) 10 mM	2.0 mM	Relative Density* (25°C, 1 bar = 1.0)	Diffusion Coefficient ($cm^2/sec \times 10^5$)
25	0.678 ± 0.006	0.226 ± 0.004	1.007	0.74† ± 0.05
70	1.04 ± 0.04	0.35 ± 0.01	0.988	1.8 ± 0.5
100	1.22 ± 0.01	0.39 ± 0.01	0.969	2.7 ± 0.1
150	1.46 ± 0.01	0.52 ± 0.01	0.930	3.8 ± 0.3
200	1.91 ± 0.02	0.62 ± 0.01	0.880	7.9 ± 0.6
250	2.21 ± 0.03	0.74 ± 0.02	0.820	12 ± 1
300	2.48 ± 0.05	0.79 ± 0.03	0.742	19 ± 3

* From Reference 20.
† From Reference 12.

Table 1: Effect of Temperature on the Diffusion Coefficient of Iodide Ions.

T (°C)	Slope of Current vs. $(Time)^{-1/2}$ ($ampere/second^{1/2} \times 10^2$) 40 mM	10 mM	Relative Density* (25°C, 1 bar = 1.0)	Diffusion Coefficient ($cm^2/sec \times 10^5$)
25	3.26 ± .04	0.84 ± .01	1.007	1.4 ± 0.1
70	4.10 ± .02	1.37 ± .01	0.988	3.2 ± 0.1
100	6.09 ± .02	1.64 ± .03	0.969	4.6 ± 0.2
150	7.84 ± .04	2.16 ± .01	0.930	9.1 ± 0.3
200	9.70 ± .04	2.48 ± .02	0.880	16 ± 1
250	9.37 ± .04	2.63 ± .08	0.820	16 ± 1
300	9.59 ± .09	2.59 ± .04	0.742	22 ± 1
350	10.19 ± .17	2.47 ± .07	0.621	37 ± 4
375	9.32 ± .27	2.53 ± .02	0.481	49 ± 9

* From Reference 20.

References.

1. Johnston, K. J. "Kirk-Othmer Encyclopedia of Chemical Technology"; Wiley: New York, 1984, 887.
2. McHugh, M. A.; "Recent Developements in Separation Science", vol. 9; Ed. Li, N. N.; Calo, J. M.; CRC Press: Boca Raton, FL, 1984.
3. Paulaitis, M. E.; Krukonis, V. J.; Kurnik, R. T.; Reid, R. C.; Reviews in Chem. Eng. 1983, 1, 179.
4. Frank, E. U.; J. Solution Chem. 1973, 2, 339.
5. Ross, D. S.; Blessing, J. E.; Nguyen, Q. C.; Hum, G. P.; Fuel 1984, 63, 1206.
6. Williams, D. F.; Chem. Eng. Sci. 1981, 36, 1769.
7. Antal, M. J.; DeAmeida, C. P.; Mok, W. S.; Ramayya, S. V.; Roy, J. C.; Paper presented at the Chicago ACS meeting, September 1985.
8. Modell, M.; U. S. Patent 4,338,199, 1982.
9. Macdonald, D. D.; "Modern Aspects of Electrochemistry", vol. 11; Ed. Conway, B. E.; Bockris, J. O'M.; Plenum Press: New York, 1975, 141.
10. McDonald, A. C.; Fan, F. F.; Bard, A. J.; J. Phys. Chem.
11. Crooks, R. M.; Fan, F. F.; Bard, A. J.; J. Am. Chem. Soc. 1984, 106, 6851.
12. Kolthoff, I. M.; Orlemann, E. F.; J. Am. Chem. Soc. 19[illegible], 63, 664.
13. Reed, T. B. "Free Energy of Formation of Binary Compounds"; MIT Press: Cambridge, MA, 1971.
14. Hoare, J. P.; J Electrochem. Soc., 1965, 112(6), 602.

15. Miles, M. H.; Kissel, G.; Lu, P, W. T.; Srinivasan, S.; J. Electrochem. Soc., 1976, 123(3), 332.

16. Gilman, S.; "Electroanalytical Chemistry", vol. 2; Ed. Bard, A. J.; Marcel Dekker, Inc.: New York, 1967.

17. Horne, R. A.; "Water and Aqueous Solutions"; John Wiley & Sons: New York, 1972, 779-82.

18. Wormald, C. J.; Ber. Bunsenges, Phys. Chem., 1984, 88, 826.

19. Tsonopoulos, C.; Wilson, G. M.; AIChE J., 1983, 29(6), 990.

20. Gmelin's; "Handbuch der Anorganischen Chemie"; Verlag Chemie, Berlin, 1931, System No. 8, 170-1.

21. Toren, E. C.; Driscoll, C. P.; Analyical Chem., 1966, 38(7), 870.

22. Bard, A. J.; Faulkner, L. R. "Electrochemical Methods, Fundimentals and Applications"; Wiley: 1980, 142-6.

23. Meyer, C. A.; McClintock, R. B.; Silvestri, G. J.; Spencer, R. C.; "ASME Steam Tables"; American Society of Mechanical Engineers: New York, 1977.

24. Lamb, W. J.; Hoffman, G. A.; Jonas, J.; J. Phys. Chem. 1981, 74, 6875.

List of Figures.

1. Diagram of high temperature, high pressure electrochemical cell. (A) 1/4" O. D. Alumina tube; (B) Hastelloy Alloy C endblock; (C) 316 S. S. Swagelok tube fitting; (D) working electrode; (E) counter electrode; (F) reference electrode; (G) electrode pressure fitting; (H) platinum coil counter electrode; (I) 316 S. S. compression fitting; (J) alumina washer; (K) fluorocarbon disk; (L) tantalum lead and platinum working electrode; (M) tantalum lead and silver reference electrode; (N) heating coil; (O) thermocouple; (P) insulation.

2. Schematic of equipment for electrochemistry in supercritical water.

3. Cyclic voltammograms of supporting electrolyte solution, 0.2 M $NaHSO_4$. Platinum working electrode, area = 1.3 * 10^{-2} cm^2. Scan rate = 5 V/S. Pressure = 240 bar. Electrode Peak identification: (A) reduction of H^+ to H_2; (B) oxidation of H_2O to O_2 and H^+; (C) oxidation of the electrode surface; (D) reduction of the electrode surface.

4. Temperature dependence of potential versus hydrogen electrode.

5. Cyclic voltammograms of 10 mM KI in 0.2 M $NaHSO_4$. Platinum working electrode, area = 1.3 * 10^{-2} cm^2. Scan rate =

5 V/S. Pressure = 240 bar. Peak identification: (A) oxidation of I- to I_2; (B) reduction of I_2 to I^-.

6. Cyclic voltammograms of 10 mM KBr in 0.2 M $NaHSO_4$. Platinum working electrode, area = 1.3 * 10^{-2} cm^2. Scan rate = 5 V/S. Pressure = 240 bar. Peak identification: (A) oxidation of Br^- to Br_2; (B) reduction of Br_2 to Br^-; (C) oxidation of the electrode surface; (D) reduction of the electrode surface; (E) oxidation of H_2O to O_2 and H^+.

7. Temperature dependence of peak potential separation in cyclic voltamograms of KI and KBr.

8. Cyclic voltammograms of 10 mM hydroquinone in 0.2 M $NaHSO_4$ and 0.5 mM KCl. Platinum working electrode, area = 1.9 * 10^{-3} cm^2. Scan rate = 5 V/S. Pressure = 240 bar. Peak identification: (A) oxidation of hydroquinone to benzoquinone; (B) reduction of benzoquinone to hydroquinone.

9. Temperature dependence of the diffusivity of iodide ions in water. Line is value calculated from Stokes-Einstein equation and the diffusity at 25°C.

10. Temperature dependence of the diffusivity of hydroquinone in water. Line is value calculated from Stokes-Einstein equation and the diffusity at 25°C.

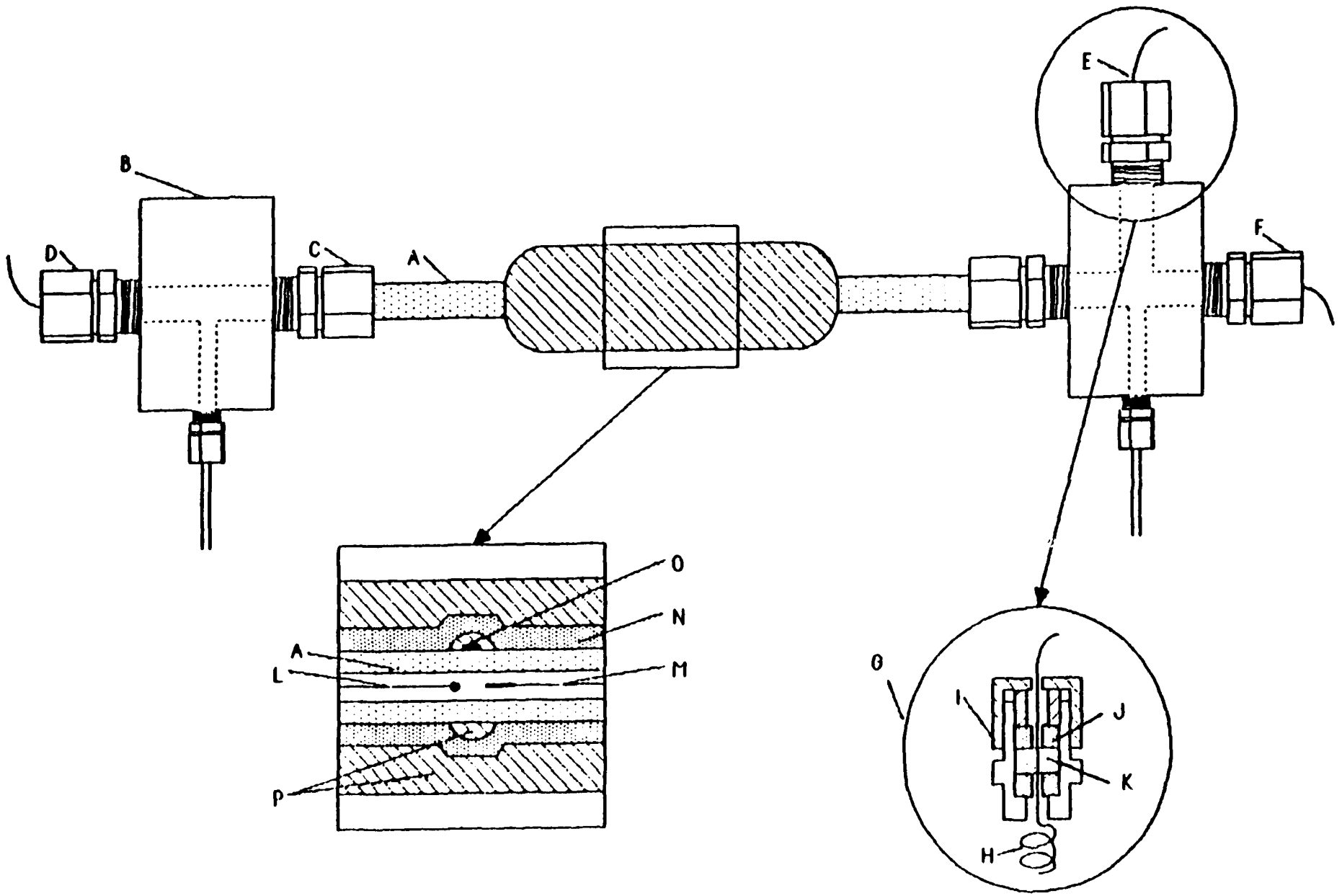

Fig. 1

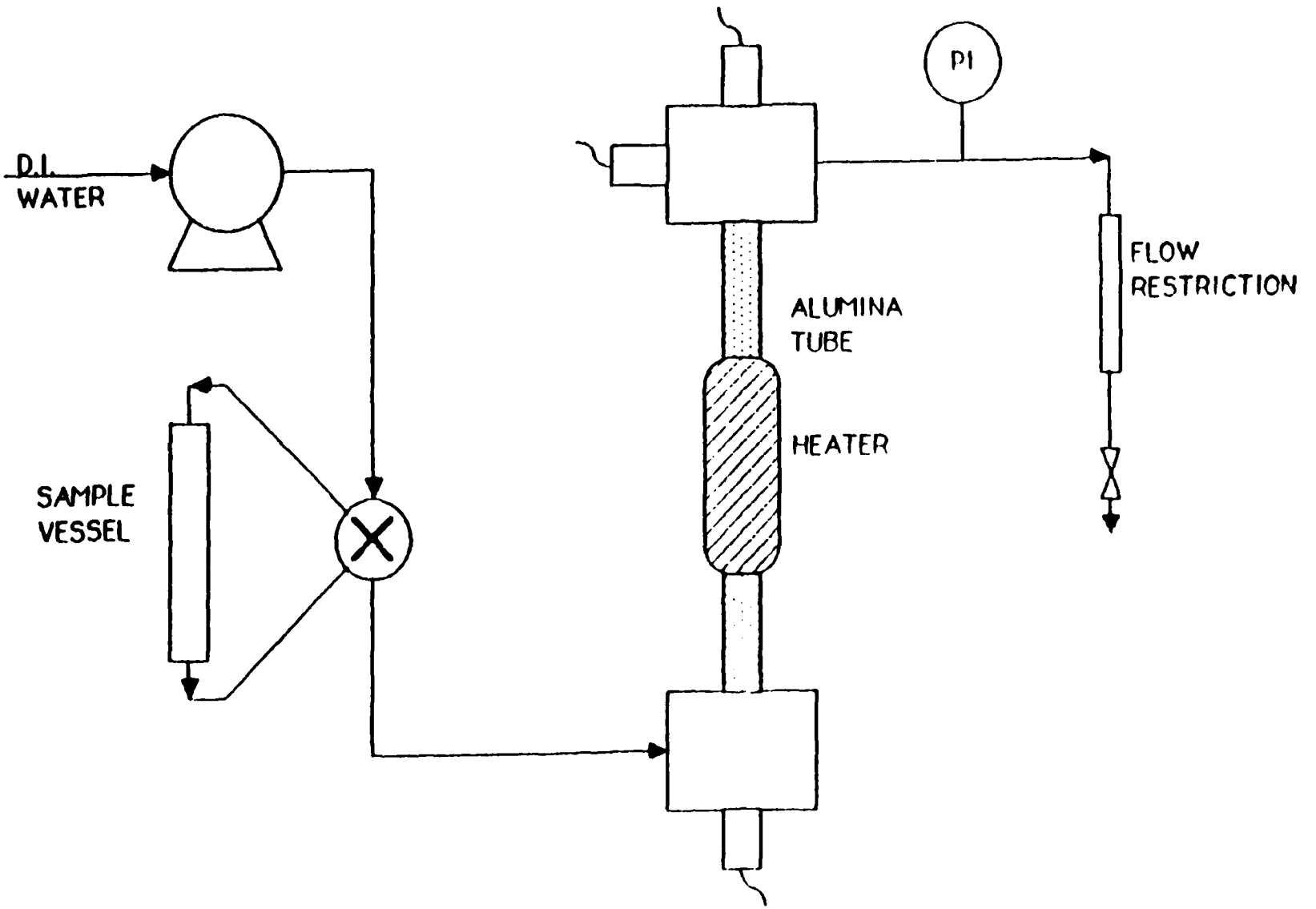
D.I.
WATER
SAMPLE
VESSEL
P1
ALUMINA
TUBE
HEATER
FLOW
RESTRICTION

Fig 2

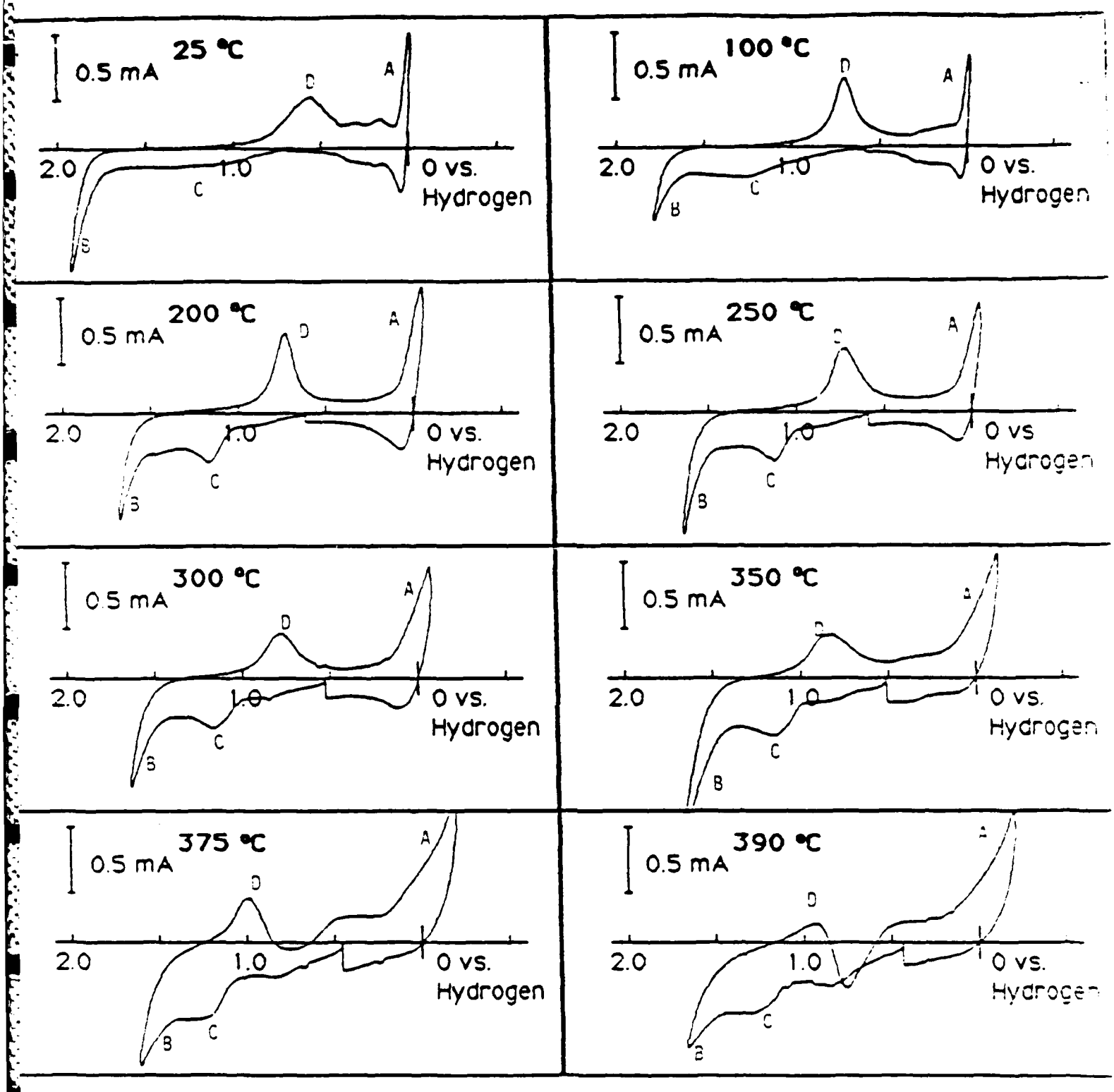
0.5 mA
25 °C
D
A
2.0
1.0
C
B
0 vs.
Hydrogen
0.5 mA
100 °C
D
A
2.0
1.0
C
B
0 vs.
Hydrogen
0.5 mA
200 °C
D
A
2.0
1.0
C
B
0 vs.
Hydrogen
0.5 mA
250 °C
D
A
2.0
1.0
C
B
0 vs
Hydrogen
0.5 mA
300 °C
A
D
2.0
1.0
C
B
0 vs.
Hydrogen
0.5 mA
350 °C
A
D
2.0
1.0
C
B
0 vs.
Hydrogen
0.5 mA
375 °C
A
D
2.0
1.0
C
B
0 vs.
Hydrogen
0.5 mA
390 °C
A
D
2.0
1.0
C
B
0 vs.
Hydrogen

Fig. 3

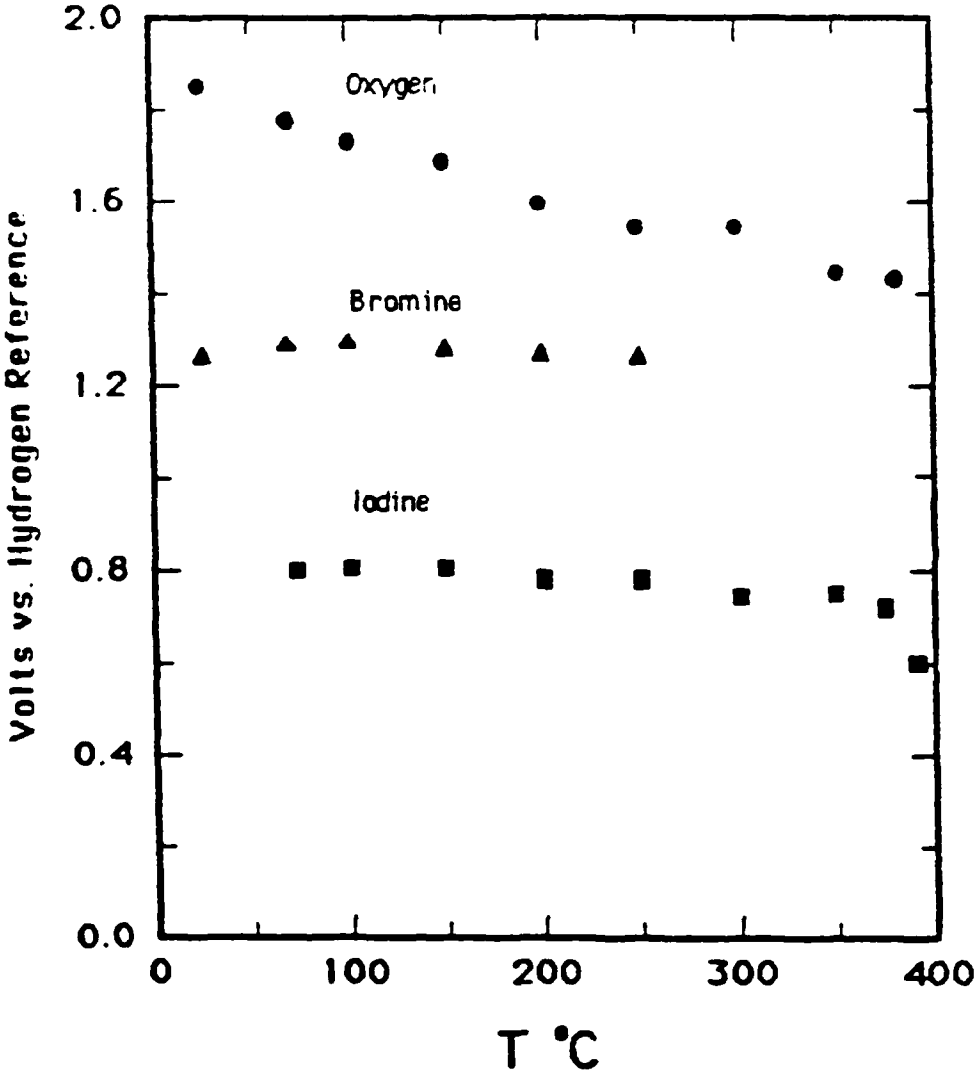
2.0
1.6
1.2
0.8
0.4
0.0
Volts vs. Hydrogen Reference
Oxygen
Bromine
Iodine
0
100
200
300
400
T °C

Fig. 4

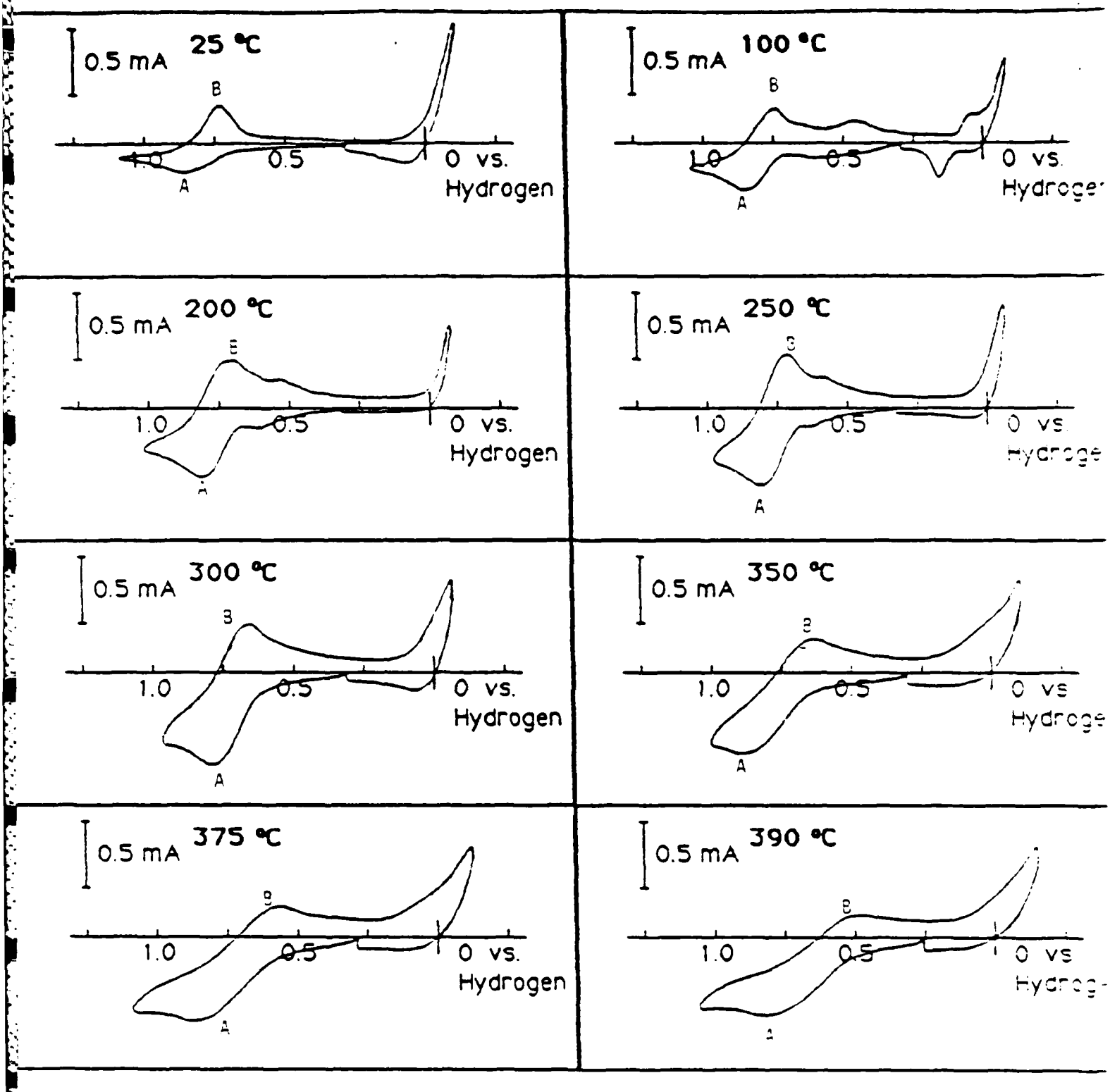
0.5 mA
25 °C
B
A
0.5
0 vs.
Hydrogen
0.5 mA
100 °C
B
A
1.0
0.5
0 vs.
Hydroge
0.5 mA
200 °C
B
A
1.0
0.5
0 vs.
Hydrogen
0.5 mA
250 °C
B
A
1.0
0.5
0 vs.
Hydroge
0.5 mA
300 °C
B
A
1.0
0.5
0 vs.
Hydrogen
0.5 mA
350 °C
B
A
1.0
0.5
0 vs
Hydroge
0.5 mA
375 °C
B
A
1.0
0.5
0 vs.
Hydrogen
0.5 mA
390 °C
B
A
1.0
0.5
0 vs
Hydroge

Fig. 5

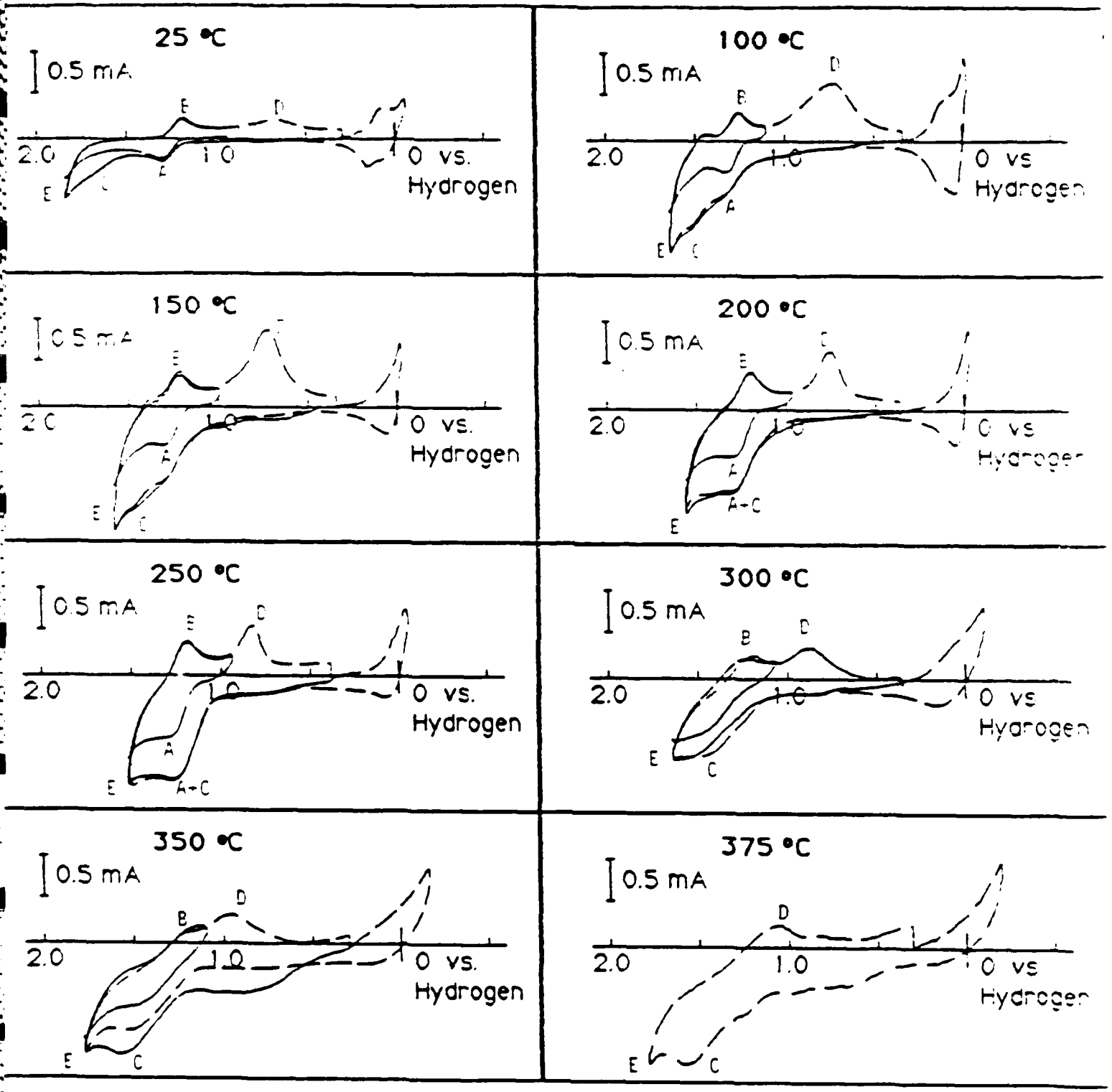
25 °C
0.5 mA
2.0
1.0
0 vs. Hydrogen
100 °C
0.5 mA
2.0
1.0
0 vs Hydrogen
150 °C
0.5 mA
2.0
1.0
0 vs. Hydrogen
200 °C
0.5 mA
2.0
1.0
0 vs Hydrogen
250 °C
0.5 mA
2.0
1.0
0 vs. Hydrogen
300 °C
0.5 mA
2.0
1.0
0 vs Hydrogen
350 °C
0.5 mA
2.0
1.0
0 vs. Hydrogen
375 °C
0.5 mA
2.0
1.0
0 vs Hydrogen

Fig. 6

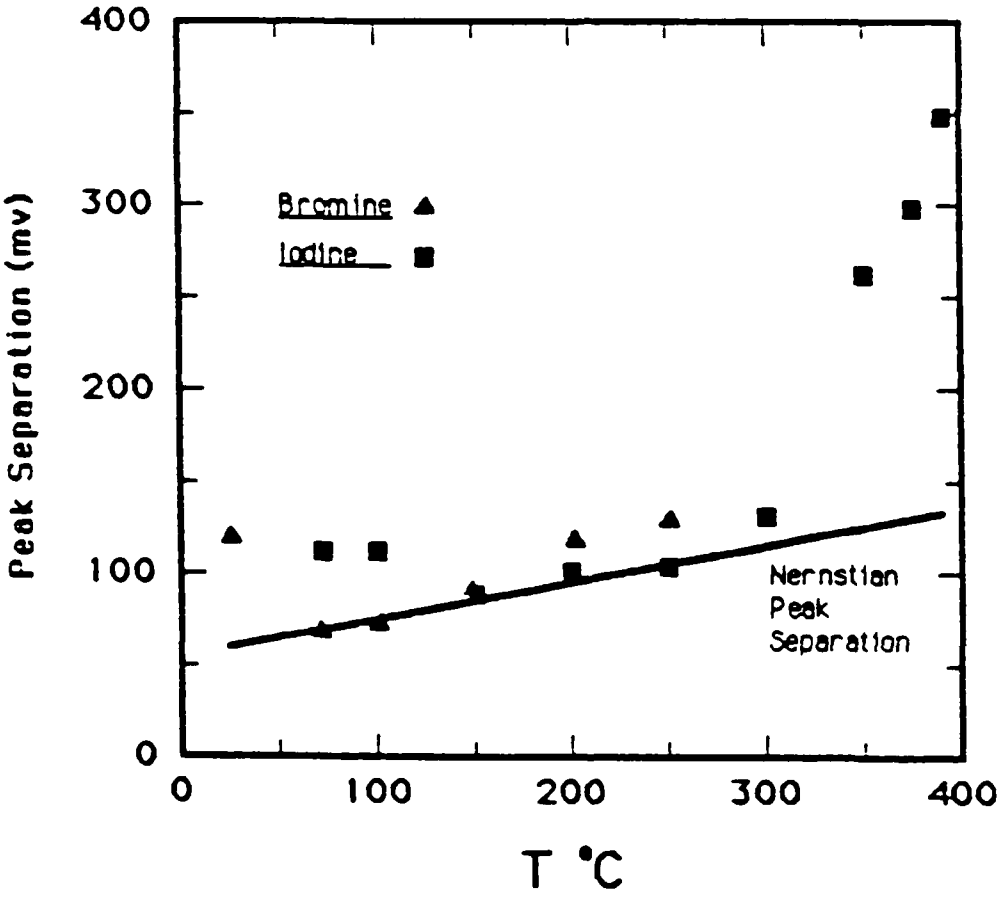
400
300
200
100
0
Peak Separation (mv)
Bromine
Iodine
Nernstian
Peak
Separation
0
100
200
300
400
T °C

Fig. 7

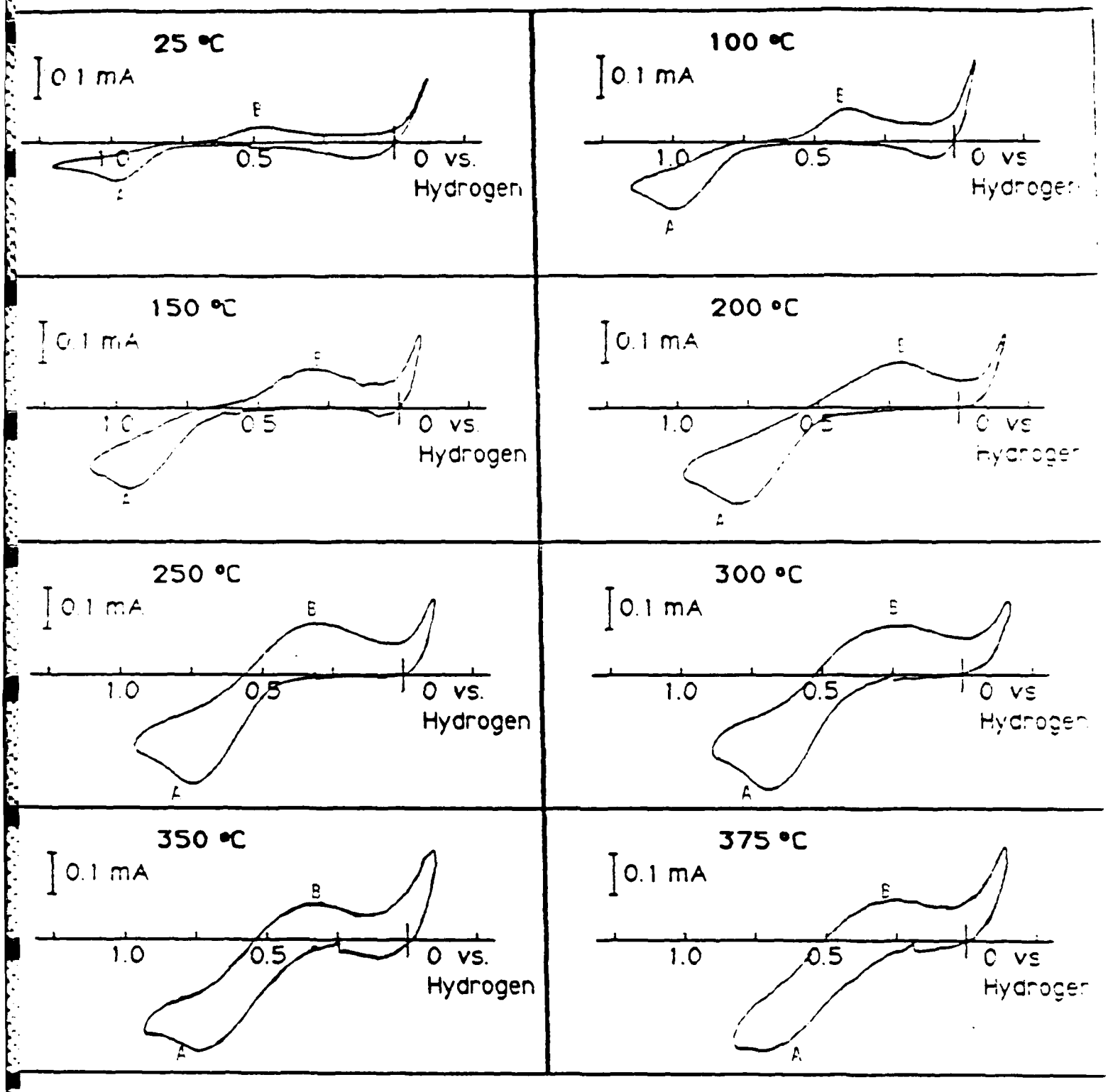
25 °C
0.1 mA
B
1.0
0.5
0 vs.
Hydrogen
A
100 °C
0.1 mA
B
1.0
0.5
0 vs
Hydrogen
A
150 °C
0.1 mA
B
1.0
0.5
0 vs.
Hydrogen
A
200 °C
0.1 mA
B
1.0
0.5
0 vs
Hydrogen
A
250 °C
0.1 mA
B
1.0
0.5
0 vs.
Hydrogen
A
300 °C
0.1 mA
B
1.0
0.5
0 vs
Hydrogen
A
350 °C
0.1 mA
B
1.0
0.5
0 vs.
Hydrogen
A
375 °C
0.1 mA
B
1.0
0.5
0 vs
Hydrogen
A

Fig 8

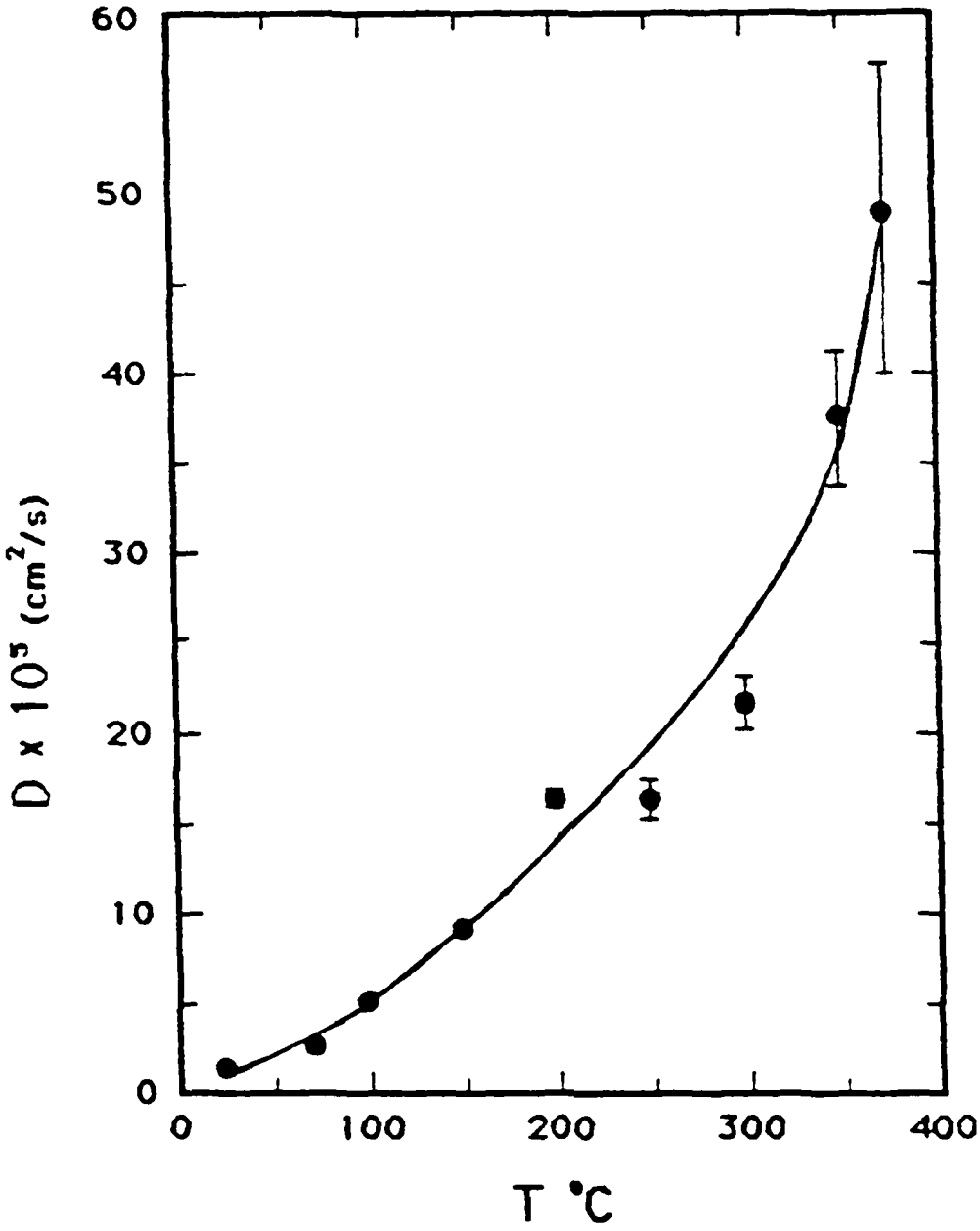

Fig. 9

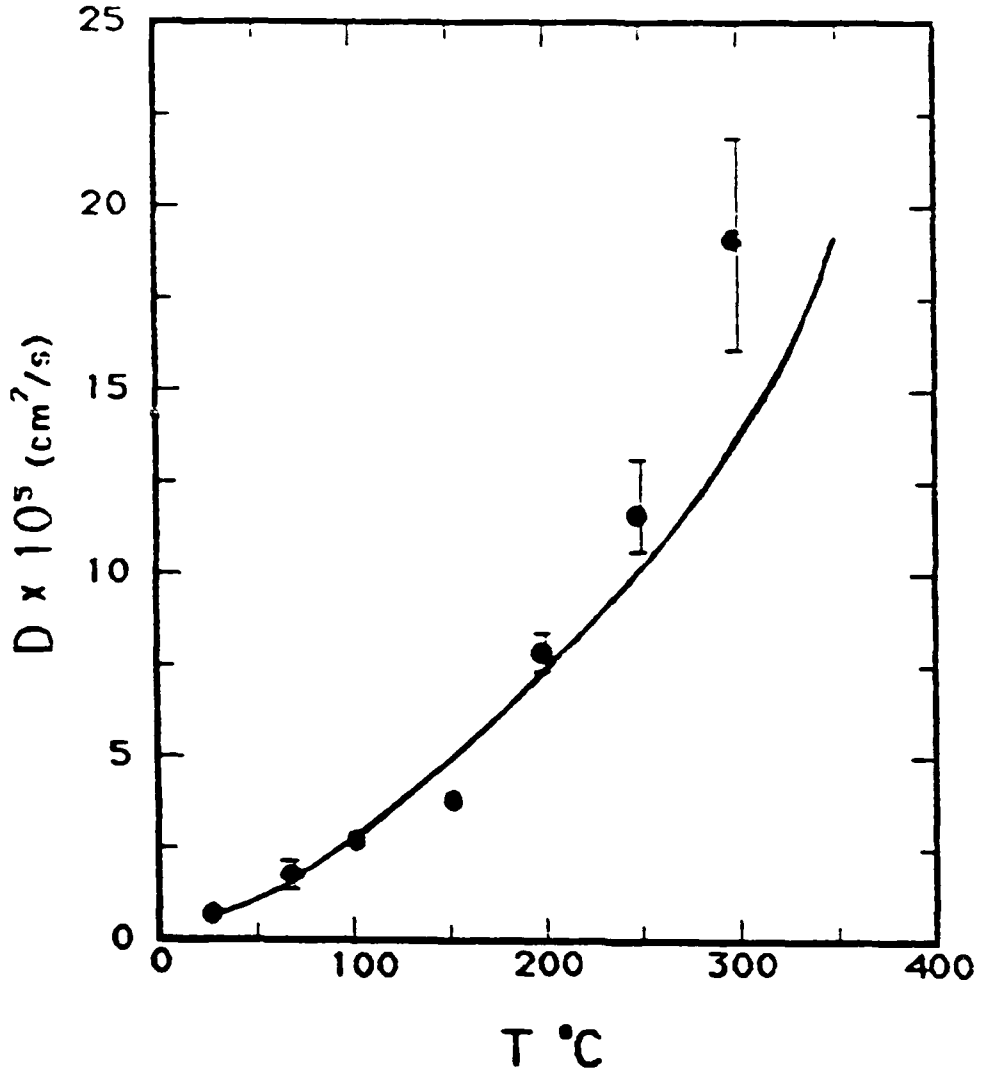

Fig. 10

END

DTIC

7-86